# Effects of wave potential on electron holes in thermal and superthermal space plasmas

Harikrishnan Aravindakshan,[a] Amar Kakad,[b] and Bharati Kakad[c]
*Indian Institute of Geomagnetism, New Panvel, Navi Mumbai 410218, India*

(Received 30 June 2018; accepted 12 November 2018; published online 6 December 2018)

Observations from various interplanetary and other spacecraft missions evince that superthermal distributions are omnipresent in the solar wind and near Earth's plasma environment. These observations confirm the presence of coherent bipolar electric field pulses. In phase space, these electric field structures are observed as electron holes (EHs) or ion holes. Trapping of particles in a potential well causes the formation of such structures and is generally studied using the Bernstein-Greene-Kruskal approach. The literature on these structures encompasses the trapped electron distribution function and physically plausible regions. In this paper, we focus on the effects of the width and amplitude of wave potential on electron trapping in thermal and superthermal plasmas. It can be observed that both an increase in the width and the amplitude of wave potential cause an augmentation in the trapping of particles. The amplitude plays a dominant role in the trapping of maximum energetic particles, whereas the width plays a role in deciding the density of particles at the center of the EHs. We found that there exists an upper limit for the stability region of EHs defined by the width-amplitude relation. Additionally, it is noticed that the superthermal plasma does not impose restriction on the presence of electron holes with a width less than the electron Debye length. *Published by AIP Publishing.* https://doi.org/10.1063/1.5046721

## I. INTRODUCTION

In the largest space plasma laboratory, the near Earth's plasma environment, there are frequent detections of coherent bipolar electric field structures by various spacecraft.[1–6] In the literature, such electric field structures are interpreted in terms of Bernstein-Greene-Kruskal (BGK) equilibrium.[7,8] Such equilibrium is formed between the particles that get trapped in the potential associated with these electric field structures and the ones those pass. The particles that are trapped will oscillate in the potential and are observed as holes in phase space. Depending on the type of particle that is trapped (electron/ion), the holes are interpreted as electron holes (EHs) or ion holes (IHs).[9]

When the solar wind plasma with high-energy particles in abundance impinges on the Earth's magnetosphere, a large amount of energy is transferred to the magnetosphere, forcing the plasma to deviate from thermal equilibrium. As the density of plasma is very low in the magnetosphere, the one-to-one binary collisions are rare. Thus, the system is less likely to attain thermal equilibrium. Thus, the distribution function of the plasma itself changes, and this ends up in different equilibriums generally called superthermal distribution.[10] The spacecraft observations suggest that the kappa distribution function is best fitted to such observations.[11] Some of the studies proposed that the nonlinear wave-particle interactions can lead to the electron kappa velocity distribution function in space plasma.[12–15] Such distributions have non-vanishing tails representing the class of energetic particles. The one-dimensional isotropic kappa velocity distribution function for electrons has the following form:[16]

$$f_e(V) = \frac{n_{0e}}{(\pi\kappa\theta_e^2)^{1/2}} \frac{\Gamma(\kappa)}{\Gamma(\kappa - 1/2)} \left[1 + \frac{V^2}{\kappa\theta_e^2}\right]^{-\kappa}. \quad (1)$$

In the equation above, $\Gamma$ is the gamma function, and $n_{0e}$ and $V$ are the density and velocity of the electrons. $\theta_e^2 = [(\kappa - 3/2)/\kappa]v_{th,e}^2$ is the most probable speed or characteristic speed, where $v_{th,e} = (2k_BT_e/m_e)^{1/2}$ is the thermal speed of the electrons and $k_B$ is the Boltzmann constant. $T_e$ and $m_e$ are the temperature and mass of the electrons. The spectral index $\kappa$ decides the slope of the tail of the distribution function, and it is always greater than 1.5. The smaller values of $\kappa$ enhance the superthermal population in the system, which lead to a decrease in the slope of the tail. As the kappa index tends to infinity ($\kappa \to \infty$), the kappa distribution function converges to the Maxwellian distribution function. For the space plasmas,[10] the kappa index is observed in the range of $2 < \kappa < 6$. The presence of superthermal particles in space plasmas indicates the need to explore the existence domain and characteristics of electrostatic solitary waves (ESWs), which is confirmed by different fluid models.[17–20] The kinetic aspects of these solitary wave structures in superthermal plasmas are not explored so far using either theory or simulations. Some seminal works have done resorting to the assumption of the background plasma to follow the thermal distribution.[21–26] However, often, it is not a feasible assumption as non-thermal distributions (like kappa) are widely observed in space plasmas. Recently, Aravindakshan *et al.*[27] have developed the BGK theory of EHs by incorporating the superthermal plasma distribution. They have given a lower

[a]harikrishnan15@iigs.iigm.res.in
[b]amar@iigs.iigm.res.in
[c]ebharati@iigs.iigm.res.in

bound for the allowed region of the width and amplitude combinations for the existence of physically plausible EHs in the superthermal plasmas.

In this paper, we investigate the behavioral change in the equilibrium solution by varying the wave potential parameters such as width and amplitude. The parametric analysis leads us to propose an upper bound for the width-amplitude combinations for the existence of stable EHs in the thermal and superthermal plasmas. In addition, we have also studied the effects of the superthermal index, $\kappa$, on the equilibrium solutions by comparing it with the thermal plasma. This paper is organized as follows: Section II discusses the mathematical formulation of the BGK theory for superthermal plasmas. Section III includes results and discussions, and concluding remarks are given in Sec. IV.

## II. MODEL

We consider a one-dimensional collisionless two-component unmagnetized plasma consisting of electrons and ions. The ions are assumed not to take part in the dynamics, and hence, they form the uniform background density. In order to study the equilibrium solution, we go to the wave frame, where our fundamental equation, Vlasov equation, loses its time dependence.[28] Hence, the time independent coupled Vlasov and Poisson equations, respectively, take the following forms:

$$v\frac{\partial f_e(v,x)}{\partial x}+\frac{1}{2}\frac{\partial \phi}{\partial x}\frac{\partial f_e(v,x)}{\partial v}=0, \tag{2}$$

$$\frac{d^2\phi}{dx^2}=\int_{-\infty}^{\infty} f_e(v,x)dv-1. \tag{3}$$

Here, $\phi$ is the wave potential formed as a result of some wave processes in plasma, which is normalized by $k_BT_e/e$. The trapped electrons in this potential form the equilibrium solution. In Eq. (3), we have used $n_e=\int_{-\infty}^{\infty} f_e(x,v)dv$ as the total number of electrons. Also, in the above equations, $v$ is the normalized electron velocity in the frame co-moving with the wave potential and $f_e$ is the electron distribution function, which is assumed to be the kappa distribution function that fills the entire system. The normalizations used here are such that the energies are normalized by ambient electron thermal energy, $2k_BT_e$. $x$ is normalized by the electron Debye length, $\lambda_{De}=\sqrt{k_BT_e/\epsilon_0 n_0 e^2}$. The velocity is normalized with electron thermal velocity $v_{th,e}=\sqrt{2k_BT_e/m_e}$. Here, we assume that the electrons follow the kappa distribution. We transformed the equations to energy frame $w$ such that $2w=v^2-\phi$. In this frame, the time dependence vanishes, and the entire calculation is done in a steady state. In such a frame, Eq. (3) can be rewritten as

$$\frac{d^2\phi}{dx^2}=\int_0^{\infty}\frac{f_p(w)}{\sqrt{2w+\phi}}dw+\int_{-\phi/2}^{0}\frac{f_{tr}(w)}{\sqrt{2w+\phi}}dw-1, \tag{4}$$

where $f_p(w)$ and $f_{tr}(w)$ are the passing and trapped particle distribution functions in the energy frame. Many spacecraft observations have observed the localized bipolar electric field structures in the Earth's magnetosphere.[1,29,30] Mostly, these bipolar pulses can be associated with the wave potential structures of the Gaussian form.[29,30] The numerical simulations shed light on the generation mechanism of these potential structures in plasma. The streaming instabilities such as two stream instability and electron beam instability can provide a great source of free energy, resulting in the formation of such potential structures.[31,32] Here, we assume a positive Gaussian type wave potential given by

$$\phi(x)=\psi\exp\left(-\frac{x^2}{2\delta^2}\right), \tag{5}$$

where $\psi$ is the amplitude of the perturbation and $\delta$ is the width of the wave potential. The expression for trapped particle density can be obtained by rearranging Eq. (4) given by

$$n_{tr}=\int_{-\phi/2}^{0}\frac{f_{tr}(w)}{\sqrt{2w+\phi}}dw=\frac{d^2\phi}{dx^2}-\int_0^{\infty}\frac{f_p(w)}{\sqrt{2w+\phi}}dw+1. \tag{6}$$

The second term in the RHS of the above equation is the passing electron density and is given by

$$\begin{aligned} n_p&=\int_0^{\infty}\frac{f_p(w)}{\sqrt{2w+\phi}}dw\\ &=\frac{AB^{\kappa}}{\sqrt{B}}\left[\frac{B^{1/2-\kappa}}{A}-2B^{-k}\phi^{1/2}\,{}_2F_1[\kappa,1/2,3/2;-\phi/B]\right], \end{aligned} \tag{7}$$

where

$$A=\frac{\Gamma(\kappa)}{\Gamma(k-1/2)\sqrt{\pi}},$$
$$B=\kappa-3/2,$$

$n_p$ is the passing electron density, and ${}_2F_1[a,b,c;z]$ is the Gauss hypergeometric function.

Substituting Eq. (7) into Eq. (6), we get the trapped electron density given by

$$\begin{aligned} n_{tr}&=\int_{-\phi/2}^{0}\frac{f_{tr}(w)}{\sqrt{2w+\phi}}dw=\frac{x^2\phi}{\delta^4}-\frac{\phi}{\delta^2}+1\\ &\quad-\frac{AB^{\kappa}}{\sqrt{B}}\left[\frac{B^{1/2-\kappa}}{A}-2B^{-k}\phi^{1/2}\,{}_2F_1[\kappa,1/2,3/2;-\phi/B]\right]. \end{aligned} \tag{8}$$

Now, our aim is to find the trapped electron distribution function. For that we need to solve the integral equation given by

$$2\int_{-\phi/2}^{0}\frac{f_{tr}(w)}{\sqrt{2w+\phi}}dw=ntr(\phi). \tag{9}$$

The solution of such an integral equation results in the expression of $f_{tr}(w)$ given by[27]

$$\begin{aligned} f_{tr}(w)&=\frac{2\sqrt{2}\sqrt{-w}}{\pi\delta^2}[1-2\ln(-8w/\psi)]\\ &\quad+\frac{A}{\sqrt{B}}\,{}_2F_1[1/2,\kappa,1;2w/B]. \end{aligned} \tag{10}$$

This is the distribution function for trapped electrons. A close look at the expression will reveal the fact that it has two parts: the first part containing the logarithmic term stems from the total charge density and the other term results from the passing electrons. In the energy frame, the negative energy (ranging from $-\phi$ to 0) is associated with trapped electrons and the positive energy (ranging from 0 to $\infty$) is associated with passing electrons. Hence, the boundary that separates passing and trapped particles is at $w=0$. It can be noticed that the trapped electron distribution function takes the indeterminate form at the boundary. We know that to be a legitimate probability distribution function representing a physical system, it should be continuous and an element of real space whose range is confined in [0, 1].[33] Hence, we redefine the domain from $[-\phi, 0]$ to $[-\phi, 0)$. This implies that the trapped particles are not present exactly at the boundaries of the potential. Thus, it can also be inferred that the turning points of particles trapped inside the potential are mostly occur at lower energies and not exactly at the boundaries.

As mentioned above, the trapped particle distribution function should be positive to form a non-vanishing BGK mode. This condition is used to derive the lower bound of the width-amplitude relationship. This relationship provides us the set of width and amplitude of wave potential which results in physically plausible BGK solutions. The width-amplitude relationship for the superthermal plasma is given by[27]

$$\delta^2 \geq \frac{2\sqrt{B}}{\pi A}\frac{\sqrt{\psi}(2ln4-1)}{{}_2F_1[1/2,\kappa,1,-\psi/B]}. \tag{11}$$

We closely analyze this expression and observe that for a specific $\psi$, there is a critical value of $\delta$ below which a stable BGK solution fails to exist. In other words, we can say that there exists a lower bound in $\delta$ for a specific $\psi$. This equation manifests that if the generated potential structure has the width and amplitude from the area where this inequality is satisfied, we get a positive $f_{tr}(w)$. Such solutions are physically realizable, and we term them as stable BGK solutions; else, the trapped electron distribution function will be negative which is physically unrealizable. Such solutions are termed as unstable BGK solutions.

## III. RESULTS AND DISCUSSION

As mentioned earlier, the kappa distribution is quite common in the near Earth's plasma environment. The bipolar electric field pulses often observed in such regions[1] are studied using the BGK theory developed for thermal plasmas.[22,34] The details of the development of BGK theory for superthermal plasmas, discussed in Sec. II, are given by Aravindakshan *et al.*[27] These authors have shown the differences in the existence domain of physically plausible BGK solutions for thermal and superthermal plasmas. We focus on the detailed study of wave potential effects on EHs formed in these kind of plasmas, which is discussed in Secs. III A–III C.

### A. Effects of the amplitude and width of wave potential on EHs

A charged particle moving in the vicinity of a potential well can have two kinds of orbits: passing particles, those particles with open orbits executing an infinite motion, and trapped particles, those move in closed finite orbits. Therefore, trapping is decided by the wave-potential that is encountered by these particles. Thus, the width and amplitude of the potential structure can influence particle trapping, which is investigated here. It may be noted that the wave potential [Eq. (5)] considered in the theoretical development of the aforementioned BGK theory gives the potential structure which has achieved a stability after trapping. So, the amplitude and width of wave potential represent the amplitude and width of the potential structure associated with EHs. We first examined the effects of the amplitude of wave potential on the thermal and superthermal plasmas by taking the constant width of the wave potential, which are shown in Fig. 1. The top panels show the effects of $\psi$ on trapped and passing particle densities defined by Eqs. (7) and (8). These equations show the distribution of trapped and passing electrons in Euclidean space. In Fig. 1, the solid (dotted) lines limn the superthermal (thermal) plasma case. The entire real space ranges from two ends of the real axis, and the passing population exists everywhere except in some regions where we expect to see global minima for the passing density. However, in such regions in the real space, the trapping populations will be a finite positive value other than zero. In Fig. 1, it is interesting to note that at the center, $x=0$, we see a local minimum in the trapped density profile. In addition, this local minimum vanishes as we decrease the amplitude of wave potential. This phenomenon suggests that the probability for the existence of trapped electron density is comparatively high at the center of the potential for a shallow potential. Physically, the congregation of particles near the center of the potential will be low for a deeper potential as they oscillate with high amplitude. This is delineated as the local minima in the trapped density profiles.

We have now discussed about the trapped electrons in real space. The oscillatory motion of such electrons inside the potential will result in a vortex type structure in phase space. Such a structure can be obtained by solving Eq. (10). The middle and bottom panels of Fig. 1 discuss the variation of the phase space structure with the amplitude of wave potential, $\psi$, for highly superthermal ($\kappa=2$) and weakly superthermal ($\kappa=20$) plasmas, respectively. We see from Fig. 1 that as we increase the amplitude of wave potential, there is not much change in the distribution of particles in the position (x) axis, but there is definitely a redistribution of particles in the conjugate space. Thus, as we increase $\psi$, the hole bulges out vertically. Also, if we see the effects of $\psi$ on the determination of particles at the center of the electron hole, we can see that it has a monotonic decrease. Moreover, the analysis shows that the holes in superthermal plasma swarm with the electrons at the center of the potential than the thermal plasma. This is predicted as we have seen that the superthermal plasma requires a large number of electrons to form a physically plausible BGK solution than its thermal counterpart.

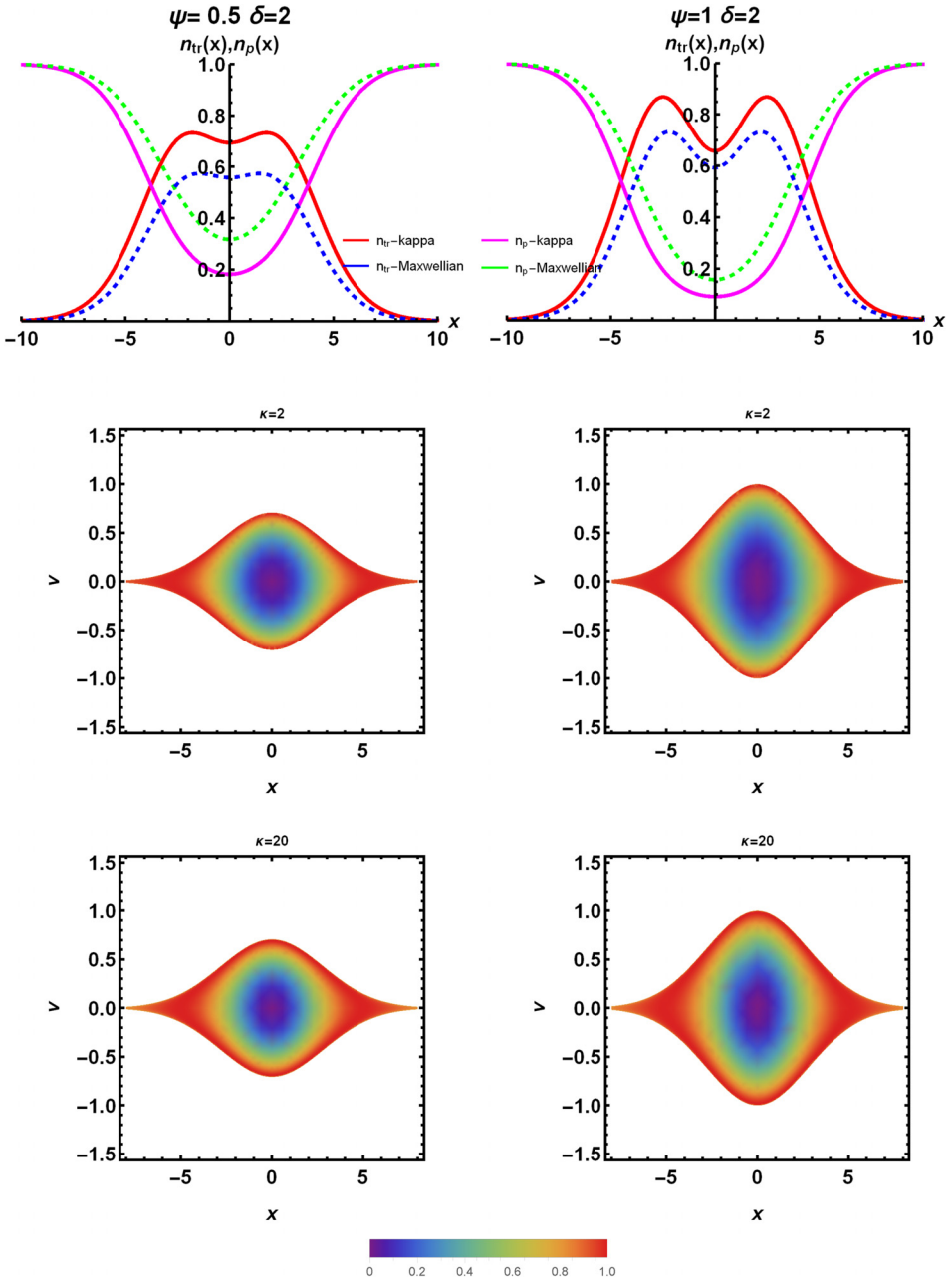


FIG. 1. The effects of amplitude of wave potential on the trapped electrons. The two plots in the top panel show the spatial distribution of trapped electron density in thermal and superthermal plasmas for different $\psi$. The dissemination of trapped electrons for thermal and superthermal plasmas is illustrated using dashed and solid lines, respectively. Here, we use $\delta = 2$ for all plots and $\psi = 0.5$ for all plots in the left panel and $\psi = 1$ and $\delta = 2$ for all plots in the right panel. For the same values of wave potential, the penultimate panel displays the phase space description of highly superthermal plasma ($\kappa = 2$), and the bottom panel shows for weakly superthermal plasma ($\kappa = 20$).

As a corollary, it can also be noticed from the trapped density profiles of Fig. 1 that the superthermal plasma shows higher trapping than the thermal plasma. This indicates that trapping is more efficient in the case of superthermal plasmas and the superthermal plasma requires a larger trapped population to form a physically plausible BGK solution. The reason for this is the average thermal energy or velocity of particles which follows the superthermal distribution ($\theta^2_{e,\kappa} = [(\kappa - 3/2)/\kappa](2k_BT_e/m_e)$) that is far less than that of the thermal plasma ($v_{th,e,M} = (2k_BT_e/m_e)^{1/2}$). As the kappa distribution function is steeper than the Maxwellian, they possess lower thermal velocity for a maximum number of particles as compared to that of Maxwellian.[16] In the case of particle trapping, particles with lower energy are likely to be trapped, whereas those with higher energy will escape from the potential. For superthermal plasmas, the number density of particles with lower thermal energy is more; hence, they should be trapped more as compared to that of thermal plasmas. We also observe that the full width at half maximum (FWHM) for superthermal plasmas is higher compared to that of thermal plasmas. The physical significance that FWHM provides is that it gives a quantified picture about the length at which the maximum trapped population is confined. Thus, for the same wave potential, the superthermal plasma will have a higher confinement length than the thermal plasma. This contradicts the current belief that the confinement length solely depends on potential applied. In addition, it is also interesting to see that (middle and bottom panels of Fig. 1) the phase space volume occupied by both thermal and superthermal plasmas is the same for a fixed wave potential. However, there are a lot more electrons trapped for superthermal plasmas. Hence, we could infer that phase space holes in superthermal plasmas are denser. In addition, they show another interesting behavior that in

comparison to the holes in thermal plasmas, holes developed in superthermal plasmas have more particles at the center.

Next, we study the effects of the width of wave potential on the EHs formed in the thermal and superthermal plasmas in Fig. 2. The top panels show the effects of $\delta$ on the trapped and passing electron densities defined by Eqs. (7) and (8), for a fixed value of $\psi$. These equations exhibit the distribution of trapped and passing electrons in Euclidean space. In Fig. 2, the solid lines symbolize the case of superthermal plasmas and the dashed lines indicate the case of thermal plasmas. As mentioned above, the trapped particle density shows a positive slope as the effect of potential begins, and at the same point, the passing density has a negative slope. In Fig. 2, it is unforeseen to note that at the center, $x = 0$, we see a local minimum in the trapped density profile. In addition, this minimum vanishes as we increase the width of wave potential. This means that the trapped electron density is comparatively low near the center of the potential. Physically, these trapped particles oscillate inside the potential. If we increase the width by keeping the amplitude constant, the trapped particles oscillate at a smaller amplitude. Hence, the probability of finding them at the center of the potential becomes high. Therefore, it is certain that we see a swarm of the trapped density at the center of the potential. We have now discussed about the trapped particles in real space. In phase space, the oscillations of these trapped particles are depicted as the vortex type structure or phase space hole. The middle and bottom panels of Fig. 2 discuss the variation of the phase space structure with the width of wave potential, $\delta$, for highly superthermal and weakly superthermal plasmas. We have used Eq. (10) to obtain the phase space plot for highly and weakly superthermal plasmas. The middle panels of Fig. 2 correspond to the case of highly superthermal plasmas ($\kappa = 2$). The case of weakly superthermal plasmas

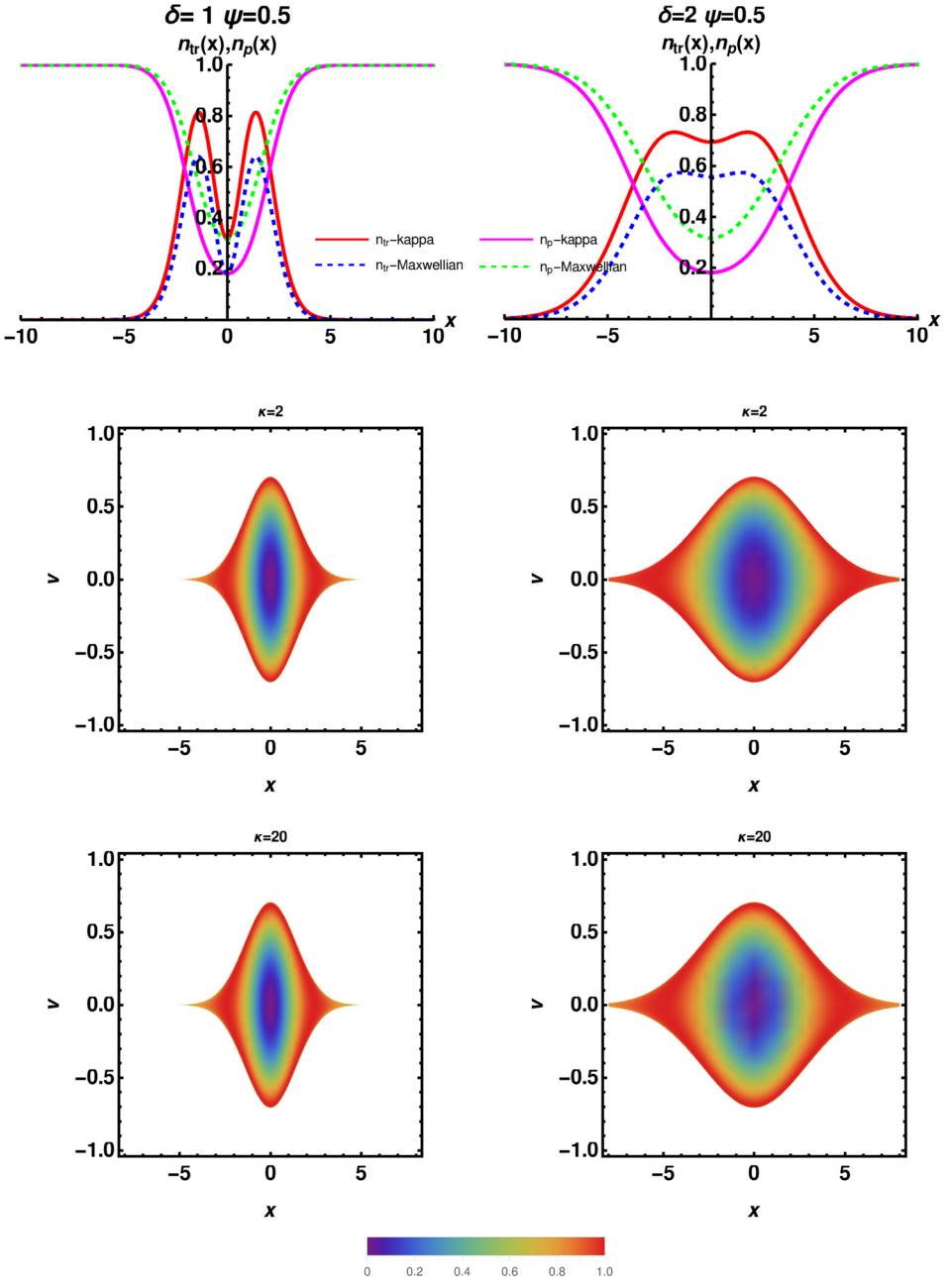


FIG. 2. The effects of the width of wave potential on the trapped electrons. The two plots in the top panel show the spatial distribution of trapped electron density for thermal and superthermal plasmas. The dissemination of trapped electrons for thermal and superthermal plasmas is illustrated using dashed and solid lines, respectively. Here, we use $\psi = 0.5$ and $\delta = 1$ for all plots in the left panel and $\psi = 0.5$ and $\delta = 2$ for all plots in the right panel. For the same values of wave potential, the penultimate panel displays the phase space description of highly superthermal plasma ($\kappa = 2$), and the bottom panel shows for weakly superthermal plasma ($\kappa = 20$).

($\kappa = 20$) is shown in the bottom panel. We see from Fig. 2 that as we increase the width of wave potential, there is no distinct change in the distribution of particles in the conjugate axis, but there is definitely a redistribution of particles in the position space. Thus, as we increase $\delta$, the hole bulges out horizontally. Also, if we analyze the effects of $\delta$ on the determination of particles near the center of electron holes, we observe that it has a monotonic increase. It can be clearly seen that the number of particles near the center of electron holes is much less for thermal plasmas. Physically speaking, potential with the larger width will have less steepness of its associated potential well, and hence, the restoring force on trapped electrons will be less. The trapped electron population near the center is determined by the restoring force, which is introduced by the steepness of the potential. If the restoring force is low, the amplitudes of the oscillation of trapped particles inside the potential well will also be lower. Hence, we see that the electrons reside mostly at the center undergoing a small simple harmonic oscillation. This could be a possible reason for the dominant electron population at the center electron holes having larger wave potential widths.

Other important feature is that trapping is higher for the EHs with larger widths. To investigate this feature in detail, we estimated total trapped particle density $n_{tr}$ by varying $\delta$ in the range of 60–4000 for different values of $\psi$ ranging from 1 to 500 in an interval of 2. As an example, the results obtained from this numerical analysis are shown in Fig. 3, where the top panels show $n_{tr}$ as a function of $\delta$ for four different values of amplitude, $\psi = 1$, 10, 100, and 500. The top left and right panels portray the case of highly and weakly superthermal plasmas, respectively. This total trapped density is obtained by integrating the trapped particle density in x-space numerically. The integration length is taken as the system length. The slope and intercept of each curve are given in the plot. The subscripts 1, 2, 3, and 4 of $m$ and $c$ indicate the slope and intercept of the curves red, magenta, blue, and green, respectively. It may be noted that the intercept for all curves is very small ($10^{-12}$ to $10^{-11}$) and can be neglected. Thus, we can say that $n_{tr} = m(\psi)\delta$, where $m$ is the slope of each curve and it is a function of $\psi$. However, we do not know the functional form of $m(\psi)$. It is evident that even though the total trapped density ($n_{tr}$) linearly increases with $\delta$, the slope of the curve has a strong dependence with $\psi$. This dependence is perused and presented in the bottom panels of Fig. 3. The dependence of the slope as a function of $\psi$ is shown by red dots, and the black line represents the nonlinear fit of the form $y = a \times \log(x) + b$, which fits the best to the data. The error in fitting is around 5%–10%. The coefficients $a$ and $b$ do vary with the $\kappa$ index, and these constants are given in Table I. The bottom left and right panels portray the case of highly and weakly superthermal plasmas, respectively. Finally, we can represent $n_{tr}$ as follows:

$$n_{tr} = [a(\kappa) + b(\kappa) \times \log(\psi)] \times \delta. \tag{12}$$

The above equation is derived from the numerical fitting of data obtained from the theoretical model. We resort to such empirical modeling because of the difficulty in the analytical integration of the trapped electron density, $n_{tr}$. We cannot get the analytical form of the $n_{tr}$ as solving these integrations analytically is difficult. Now, we see from Fig. 3 that the slope of the curve tends to saturate after certain $\psi$. Thus, it becomes apparent that for a given $\delta$, there exists a maximum value of $\psi$ after which the amplitude of wave potential affects less significantly to $n_{tr}$.

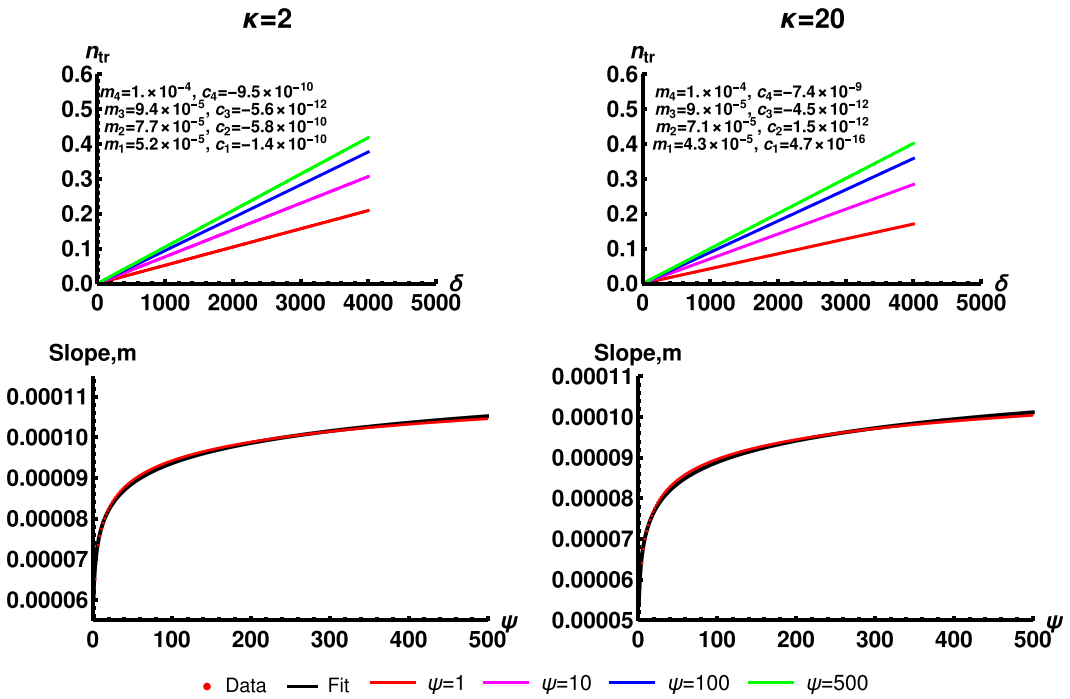


FIG. 3. The total trapped density per system length plotted as a function of the width of wave potential $\delta$ for different amplitudes, $\psi$, is given. The four panels show this variation for different superthermal indexes, $\kappa$. Here, red, magenta, blue, and green represent $\psi = 1$, 10, 100, and 500, respectively. The subscripts 1, 2, 3, and 4 of m and c indicate the slope and intercept of the curve red, magenta, blue, and green, respectively.

TABLE I. The value of constants a and b for different values of nonthermal index $\kappa$. It may be noted that $a$ and $b$ are functions of $\kappa$ and used in Eq. (12) to estimate the total trapped electron density.

| $K$ | a | b |
|---|---|---|
| 2 | $5.98 \times 10^{-5}$ | $7.19 \times 10^{-6}$ |
| 3 | $5.56 \times 10^{-5}$ | $7.45 \times 10^{-6}$ |
| 4 | $5.37 \times 10^{-5}$ | $7.56 \times 10^{-6}$ |
| 10 | $5.33 \times 10^{-5}$ | $7.60 \times 10^{-6}$ |
| 20 | $5.30 \times 10^{-5}$ | $7.62 \times 10^{-6}$ |

We know that the maximum value of $n_{tr}$ can reach up to one. It means for a given $\psi$, there exists a $\delta$ such that $n_{tr}$ is one, above which all the values of $\delta$ result in non-physical values of $n_{tr}$. Thus, this imparts an upper bound for the width-amplitude relationship.

Now, we have evinced that there exists an upper bound also for the width amplitude relationship. From the maximum value calculated from the analysis of the dependence of $n_{tr}$ with $\delta$, we saw that it has a linear dependence with the intercept to be zero. As we mentioned, the upper bound occurs when $n_{tr}$ becomes unity, i.e., the case of maximum trapping. When we use this condition in Eq. (12), we get

$$1 = [a(\kappa) + b(\kappa) \times \log(\psi)] \times \delta. \tag{13}$$

Thus, the upper bound of the width amplitude relationship turns out to be

$$\delta = [a(\kappa) + b(\kappa) \times \log(\psi)]^{-1}. \tag{14}$$

For a highly superthermal plasma, the values of $a$ and $b$ are $5.98 \times 10^{-5}$ and $7.19 \times 10^{-6}$, respectively. The values of $a$ and $b$ for different values of the superthermal index are given in Table I. Hence, the upper bound of the width amplitude limit turns out to be

$$\delta = (5.98 \times 10^{-5} + 7.19 \times 10^{-6} \times \log(\psi))^{-1}. \tag{15}$$

This is shown in Fig. 4. The first panel of this figure shows the upper bound for various superthermal indexes. It can be noted that as we move to the thermal regime, the upper bound limit of the stability region increases. This is because the stability of a BGK mode is decided by the number of trapped particles. Also, we have derived this using the condition that $n_{tr}$ attains its maximum value of one. We know that the superthermal plasma requires more trapped particles than the thermal plasma to form a physically plausible BGK mode. Hence, it is natural that the superthermal plasma attains the maximum value of $\delta$ for a specific $\psi$ at a lower point than the thermal plasma. The right top panel in Fig. 4 shows the total stability region for the highly superthermal plasma. The magenta line shows the lower bound limit, and the red line indicates the upper bound limit. The bottom panel depicts the phase space hole at the upper boundary for highly superthermal and weakly superthermal plasmas. It can be observed that at their respective upper boundary, the superthermal plasma has a larger hole and its entire particles

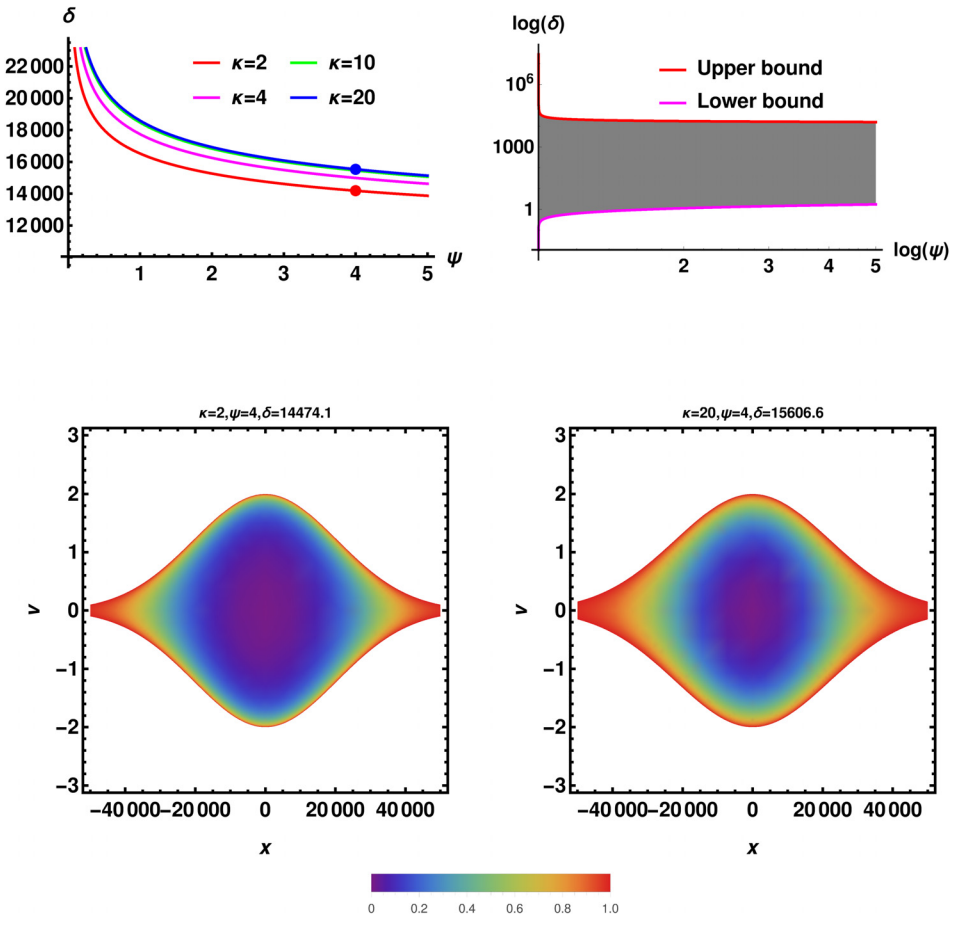


FIG. 4. The upper limit of the width amplitude relation and the corresponding phase space hole are depicted. The left top panel shows the upper limit of the width-amplitude curve for the various values of superthermal index $\kappa$. The right top panel shows the complete stability region for a highly superthermal plasma (i.e., $\kappa = 2$). The bottom panels show the space holes at the maximum allowed $\delta$ for a fixed $\psi$ for highly and weakly superthermal plasmas. The red and blue points on the left top panel show the values for which the phase space plot is drawn. The red (blue) dot indicates the case of highly (weakly) superthermal plasma $\kappa = 2$ ($\kappa = 20$).

are concentrated at the rim compared to that of the center or the inner part of the vortex compared to the thermal plasma. The upper bound implies that the physically plausible BGK solutions not only have a lower limit for their size, but they also have an upper limit.

### B. Variation in the trapped particle distribution function

Even though we have seen the effects that the amplitude and width of wave potential introduced to get a complete picture, we need to probe their effects in conjugate space also. Figure 5 portrays the effect of $\delta$ on trapping in conjugate space. We have numerically integrated the distribution function in x-space and found the variation in v-space. It can be clearly noted that as we increase $\delta$, more particles of lower velocities are trapped. It indicates that as we increase $\delta$ instead of trapping more and more higher energy particles, more and more lower energy particles are trapped. Hence, we can conclude that the width of wave potential decides the trapping density of lower energy particles. It is also interesting to note that as we go for increasing the width of wave potential, the effect of the superthermal index gains significance.

The effect of wave potential amplitude on trapping in the v-domain is shown in Fig. 6. Figure 6 shows the variation of the trapped electron distribution function in v-space for various $\psi$. It can be clearly noted that as we increase $\psi$, the particles of higher velocities are trapped, but the maximum trapping still remains the same, which can be understood by looking at the origin. It indicates that as we increase $\psi$ instead of trapping more and more lower energy particles, more and more higher energy particles are trapped. Hence, we can conclude that the amplitude of wave potential decides which is the highest velocity of particles trapped.

### C. Size of electron holes

We have seen that the lower bound of the stability regions is obtained by assuming the positivity of the trapped electron distribution function. Such a relationship is called the width-amplitude relationship given by[27]

$$\delta^2 \geq \frac{2\sqrt{B}}{\pi A}\frac{\sqrt{\psi}(2ln4-1)}{{}_2F_1[1/2,\kappa,1,-\psi/B]}. \tag{16}$$

For a highly superthermal plasma, i.e., $\kappa = 2$, this relation is given by

$$\delta \geq 1.12\left(\frac{\sqrt{\psi}(2\psi+1)^{3/2}}{\psi+1}\right)^{0.5}. \tag{17}$$

The above equation gives us the width-amplitude relationship for the highly superthermal plasma ($\kappa = 2$). We have already mentioned that $\delta$ is the width of the potential and $\psi$ is the amplitude of the potential. It can be observed that inequality in the above equation [Eq. (17)] holds for arbitrary values of $\psi$ and $\delta$. It is intuitively obvious that the size of electron holes will be less than or equal to the width of the potential. Hence, the superthermal plasma supports EHs of arbitrary size. Figure 7(a) shows the trapped density plots for both superthermal and thermal plasmas with $\delta = 0.1$ and $\psi = 2 \times 10^{-5}$. The solid line delineates the trapped density of superthermal plasmas, and the dashed lines delineate the trapped density of thermal plasmas. Figure 7(a) also shows

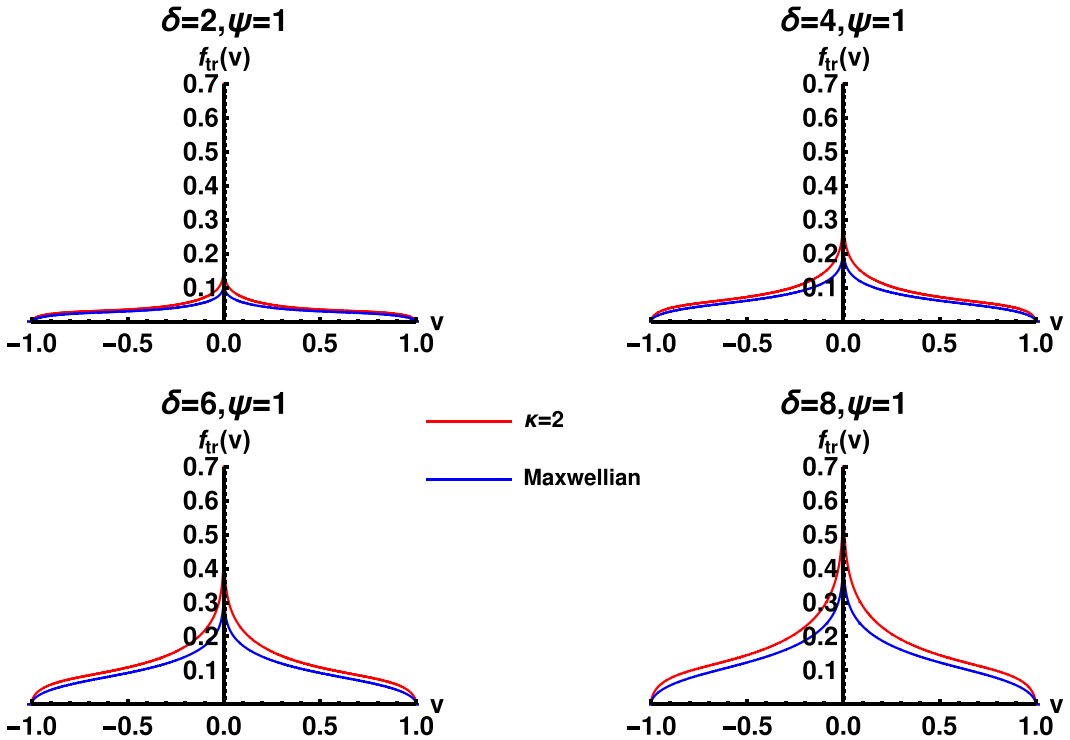


FIG. 5. The variation of the trapped electron distribution function of thermal and superthermal plasmas in velocity space for different $\delta$ is shown here. The superthermal index, $\kappa$, is set to 2, and the amplitude of the wave potential, $\psi$, is set to 1. Blue and red colors show the case of thermal and superthermal plasmas, respectively.

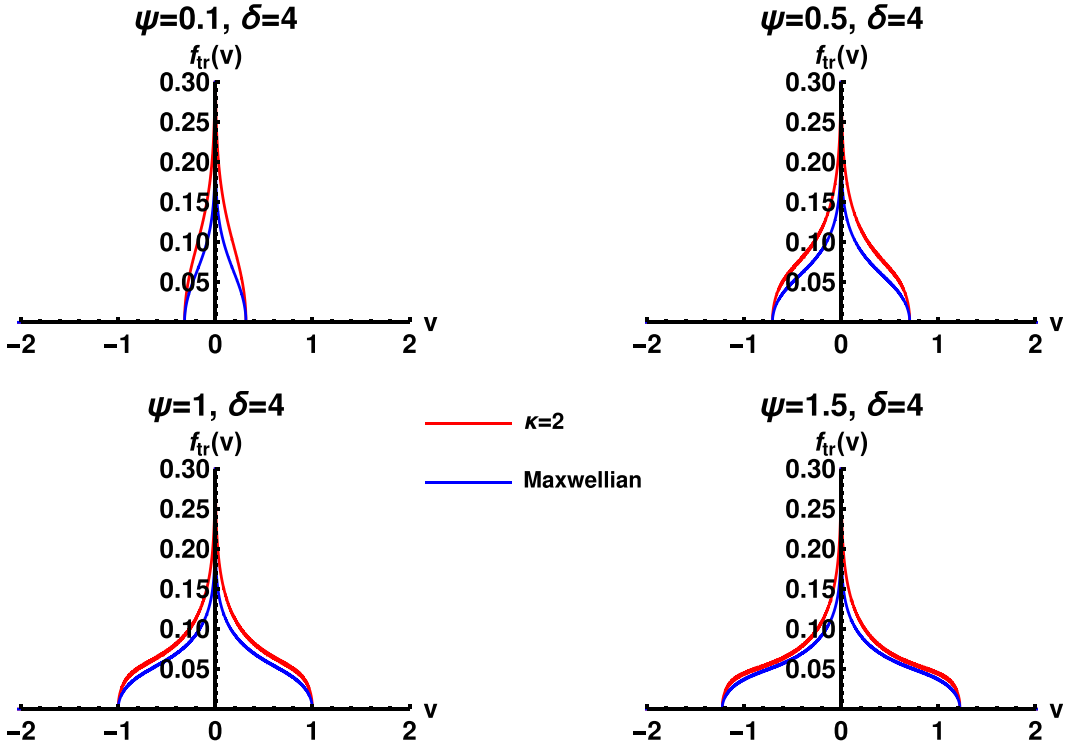


FIG. 6. The variation of the trapped electron distribution function of thermal and superthermal plasmas in velocity space for different $\psi$ is shown here. The superthermal index, $\kappa$, is set to 2, and the width of the wave potential, $\delta$, is set to 4. Blue and red colors show the case of thermal and superthermal plasmas, respectively.

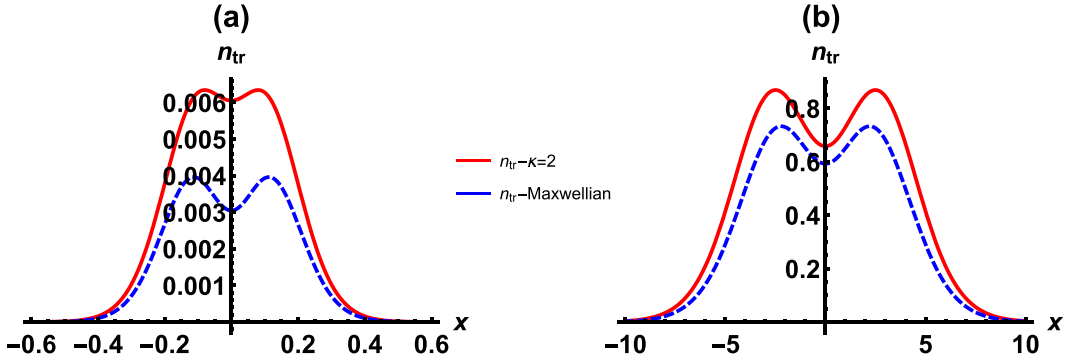


FIG. 7. The trapped particle density for small and large wave potentials. (a) The case of small wave potential with the amplitude of wave potential, $\psi = 2 \times 10^{-5}$, and the width of wave potential, $\delta = 0.1$, for thermal and superthermal plasmas. (b) The case of large wave potential with the amplitude of wave potential, $\psi = 1$, and the width of wave potential, $\delta = 2$, for thermal and superthermal plasmas.

that the entire charge density is confined within one $\lambda_{De}$. This demonstrates that the superthermal plasmas also support EHs of arbitrary size theoretically. It is well known that the Debye length has a direct dependence with the superthermal index.[35,36] Hence, a positive core is screened out at a shorter distance than the thermal plasma. The electrons trapped inside the potential oscillate inside the potential well about the positive core. The spatial scale length in the phase space plot or the trapped density profile clearly shows that the size of the hole is less than one $\lambda_{De}$. As the combination of $\psi$ and $\delta$, i.e., the amplitude and width of wave potential, respectively, is chosen from the allowed region, it is explicit that like thermal plasmas, superthermal plasmas also support EHs of size less than the Debye length and the positive core is screened by the oscillation of trapped electrons as suggested by Chen.[34] This again substantiates the fact that more particles will be trapped in the superthermal plasma.

As we go on increasing the wave potential, the confinement length also increases. This is shown in Fig. 7(b), where $\delta = 2$ and $\psi = 1$. The solid line delineates the trapped density of superthermal plasma, and the dashed lines delineate the trapped density of thermal plasmas. It can be observed that the trapped particle density in this case is not confined within one $\lambda_{De}$.

## IV. CONCLUDING REMARKS

This paper laid down a detailed and comprehensive study of BGK theory for superthermal space plasmas by investigating the role of each physical parameter in the

theory. The main outcome of the study is that we obtained an empirical relation for the total density of trapped electrons associated with a wave potential formed in the superthermal plasmas. We found that there exists an upper bound limit for the physically plausible region of EHs in width—amplitude ($\psi - \delta$) space. It was believed earlier that the parametric space of $\psi$ and $\delta$ will have a lower bound above which the physically plausible BGK solutions can exist. However, we have found physically that plausible BGK solutions do have an upper boundary in the $\psi - \delta$ parametric region. As there is an upper limit on $\delta$ associated with physically plausible BGK solutions, it implies that there is a limit on the maximum size of EHs as well.

Second, we have studied the effect of wave potential and superthermal index on particle trapping and its distribution function. We have observed significant differences in the existence and the characteristics of EHs in thermal and superthermal plasmas. One of the most important differences is that superthermal plasma requires a higher number of trapped particles to form physically plausible BGK solutions compared to the thermal plasma. The superthermal index plays an important role in trapping as it controls the abundance of lower thermal energy particles which makes the interaction between the plasma and the wave potential stronger. We also find that the total trapped electron density is predominantly determined by the amplitude of the wave potential. In addition, the number of particles present at the center of the EHs asymptotically decreases with the amplitude of the wave potential. The reason behind this seems to be clear. As the potential has a high amplitude, it will cause the trapped electrons to oscillate faster with very high amplitude. Hence, the probability of observing the particle at the center of the EH becomes low. In contrast, the width of the potential has a negative dependence on the probability of finding particles at the center. It is also interesting to find that the amplitude of the wave potential decides the trapping of higher energy particles and the width of the wave potential decides the trapping of lower energy particles.

In a linearized theory, the minimum wave length is the Debye length[37,38] for which the plasma cannot shield out disturbances for scales smaller than the Debye radius. From the detailed analysis, we arrive at a conclusion that superthermal plasmas add no restriction on the size of EHs theoretically formed. In fact, the generation of physically plausible EHs with size less than or equal to one electron Debye length is theoretically allowed. It is known that the Debye length of the superthermal plasma is smaller than that of the Maxwellian plasma.[35,36] Chen has conjectured in her thesis[34] that the size of EHs can be less than the Debye length for thermal plasmas. They suggested that the oscillation of trapped electrons in the potential well screens out the positive potential. As the Debye length of the superthermal plasma itself is small,[35] we expect the size of electron holes to be smaller than that of the thermal plasma. In addition, we have seen that $n_{tr}$ for superthermal plasmas is higher compared to that for thermal plasmas, so the potential will be screened out at a lower length. Thus, the minimum size of EHs which is supported by the superthermal plasmas is less than that of thermal plasmas.


[1]H. Matsumoto, H. Kojima, T. Miyatake, Y. Omura, M. Okada, I. Nagano, and M. Tsutsui, "Electrostatic solitary waves (esw) in the magnetotail: Ben wave forms observed by geotail," Geophys. Res. Lett. **21**, 2915–2918, https://doi.org/10.1029/94GL01284 (1994).

[2]S. Bale, P. Kellogg, D. Larsen, R. Lin, K. Goetz, and R. Lepping, "Bipolar electrostatic structures in the shock transition region: Evidence of electron phase space holes," Geophys. Res. Lett. **25**, 2929–2932, https://doi.org/10.1029/98GL02111 (1998).

[3]H. Matsumoto, X. Deng, H. Kojima, and R. Anderson, "Observation of electrostatic solitary waves associated with reconnection on the dayside magnetopause boundary," Geophys. Res. Lett. **30**, 1326, https://doi.org/10.1029/2002GL016319 (2003).

[4]A. Kakad, S. Singh, R. Reddy, G. Lakhina, and S. Tagare, "Electron acoustic solitary waves in the earths magnetotail region," Adv. Space Res. **43**, 1945–1949 (2009).

[5]A. Kakad, B. Kakad, C. Anekallu, G. Lakhina, Y. Omura, and A. Fazakerley, "Slow electrostatic solitary waves in earth's plasma sheet boundary layer," J. Geophys. Res.: Space Phys. **121**, 4452–4465, https://doi.org/10.1002/2016JA022365 (2016).

[6]G. Lakhina, S. Singh, A. Kakad, and J. Pickett, "Generation of electrostatic solitary waves in the plasma sheet boundary layer," J. Geophys. Res.: Space Phys. **116**, A10218, https://doi.org/10.1029/2011JA016700 (2011).

[7]M. Temerin, K. Cerny, W. Lotko, and F. Mozer, "Observations of double layers and solitary waves in the auroral plasma," Phys. Rev. Lett. **48**, 1175 (1982).

[8]L. Muschietti, R. Ergun, I. Roth, and C. Carlson, "Correction to phase-space electron holes along magnetic field lines," Geophys. Res. Lett. **26**, 1689–1689, https://doi.org/10.1029/1999GL900302 (1999).

[9]I. Hutchinson, "Electron holes in phase space: What they are and why they matter," Phys. Plasmas **24**, 055601 (2017).

[10]V. Pierrard and M. Lazar, "Kappa distributions: Theory and applications in space plasmas," Sol. Phys. **267**, 153–174 (2010).

[11]V. M. Vasyliunas, "A survey of low-energy electrons in the evening sector of the magnetosphere with ogo 1 and ogo 3," J. Geophys. Res. **73**, 2839–2884, https://doi.org/10.1029/JA073i009p02839 (1968).

[12]G. Livadiotis and D. McComas, "Understanding kappa distributions: A toolbox for space science and astrophysics," Space Sci. Rev. **175**, 183–214 (2013).

[13]C.-y. Ma and D. Summers, "Formation of power-law energy spectra in space plasmas by stochastic acceleration due to whistler-mode waves," Geophys. Res. Lett. **25**, 4099–4102, https://doi.org/10.1029/1998GL900108 (1998).

[14]P. Yoon and G. Livadiotis, "Nonlinear wave–particle interaction and electron kappa distribution," in *Kappa Distributions* (Elsevier, 2017), pp. 363–398.

[15]X. Tao and Q. Lu, "Formation of electron kappa distributions due to interactions with parallel propagating whistler waves," Phys. Plasmas **21**, 022901 (2014).

[16]D. Summers and R. M. Thorne, "The modified plasma dispersion function," Phys. Fluids B **3**, 1835–1847 (1991).

[17]N. Saini, I. Kourakis, and M. Hellberg, "Arbitrary amplitude ion-acoustic solitary excitations in the presence of excess superthermal electrons," Phys. Plasmas **16**, 062903 (2009).

[18]A. Lotekar, A. Kakad, and B. Kakad, "Fluid simulation of dispersive and nondispersive ion acoustic waves in the presence of superthermal electrons," Phys. Plasmas **23**, 102108 (2016).

[19]A. Lotekar, A. Kakad, and B. Kakad, "Generation of ion acoustic solitary waves through wave breaking in superthermal plasmas," Phys. Plasmas **24**, 102127 (2017).

[20]A. Kakad, A. Lotekar, and B. Kakad, "First-ever model simulation of the new subclass of solitons supersolitons in plasma," Phys. Plasmas **23**, 110702 (2016).

[21]L.-J. Chen and G. K. Parks, "BGK electron solitary waves: 1D and 3D," Nonlinear Processes Geophys. **9**, 111–119 (2002).

[22]V. Turikov, "Electron phase space holes as localized bgk solutions," Phys. Scr. **30**, 73 (1984).

[23]I. Dodin, "On variational methods in the physics of plasma waves," Fusion Sci. Technol. **65**, 54–78 (2014).

[24]R. Berger, S. Brunner, T. Chapman, L. Divol, C. Still, and E. Valeo, "Electron and ion kinetic effects on non-linearly driven electron plasma and ion acoustic waves," Phys. Plasmas **20**, 032107 (2013).

[25]S. Brunner, R. L. Berger, B. I. Cohen, L. Hausammann, and E. J. Valeo, "Kinetic simulations and reduced modeling of longitudinal sideband instabilities in non-linear electron plasma waves," Phys. Plasmas **21**, 102104 (2014).

[26]K. Hara, T. Chapman, J. W. Banks, S. Brunner, I. Joseph, R. L. Berger, and I. D. Boyd, "Quantitative study of the trapped particle bunching instability in Langmuir waves," Phys. Plasmas **22**, 022104 (2015).
[27]H. Aravindakshan, A. Kakad, and B. Kakad, "Bernstein-Greene-Kruskal theory of electron holes in superthermal space plasma," Phys. Plasmas **25**, 052901 (2018).
[28]I. B. Bernstein, J. M. Greene, and M. D. Kruskal, "Exact nonlinear plasma oscillations," Phys. Rev. **108**, 546 (1957).
[29]R. Ergun, C. Carlson, L. Muschietti, I. Roth, and J. McFadden, "Properties of fast solitary structures," Nonlinear Processes Geophys. **6**, 187–194 (1999).
[30]R. Ergun, C. Carlson, J. McFadden, F. Mozer, L. Muschietti, I. Roth, and R. Strangeway, "Debye-scale plasma structures associated with magnetic-field-aligned electric fields," Phys. Rev. Lett. **81**, 826 (1998).
[31]Y. Omura, H. Matsumoto, T. Miyake, and H. Kojima, "Electron beam instabilities as generation mechanism of electrostatic solitary waves in the magnetotail," J. Geophys. Res.: Space Phys. **101**, 2685–2697, https://doi.org/10.1029/95JA03145 (1996).
[32]Q. Lu, D. Wang, and S. Wang, "Generation mechanism of electrostatic solitary structures in the earth's auroral region," J. Geophys. Res.: Space Phys. **110**, A03223, https://doi.org/10.1029/2004JA010739 (2005).
[33]H. L. Royden and P. Fitzpatrick, *Real Analysis* (Macmillan, New York, 1968), Vol. 2.
[34]L.-J. Chen, "Bernstein-Greene-Kruskal solitary waves in collisionless plasma," Ph.D. dissertation (Univ. of Wash., Seattle, 2002).
[35]D. A. Bryant, "Debye length in a kappa-distribution plasma," J. Plasma Phys. **56**, 87–93 (1996).
[36]G. Livadiotis and D. McComas, "Electrostatic shielding in plasmas and the physical meaning of the Debye length," J. Plasma Phys. **80**, 341–378 (2014).
[37]D. Bohm and E. P. Gross, "Theory of plasma oscillations. A. Origin of medium-like behavior," Phys. Rev. **75**, 1851–1864 (1949).
[38]I. Langmuir, "Oscillations in ionized gases," Proc. Natl. Acad. Sci. U. S. A. **14**, 627–637 (1928).